

Optimal Design of HGV Front Structure for Pedestrian Safety

著者	Ramli Faiz Redza, Yamazaki Koetsu
journal or publication title	Journal of Advanced Mechanical Design, Systems, and Manufacturing
volume	6
number	4
page range	541-557
year	2012-01-01
URL	http://hdl.handle.net/2297/36510

doi: 10.1299/jamdsm.6.541

Optimal Design of HGV Front Structure for Pedestrian Safety*

Faiz Redza RAMLI** and Koetsu YAMAZAKI**

**Kanazawa University, Kakuma-machi, Kanazawa, 920-1192, Japan

E-mail: faredza@stu.kanazawa-u.ac.jp

Abstract

This paper addresses a pedestrian safety design of front structure of Heavy Goods Vehicle (HGV) by two concepts; firstly by equipping a lower bumper stiffener structure under the front bumper and secondly by putting an airbag in front of the HGV front panel. In this study, HGV-pedestrian collision accident was simulated by the crash analysis solver MADYMO environment, where the HGV model with the speed of 20 km/h was collided with an adult male and with an adult female pedestrian, respectively. The bumper and lower bumper stiffener were varied their positions, while the airbag was adjusted the vent hole size and the position of airbag in front of front panel vertically. The pedestrian injuries that can be sustained during the simulation impact were limited at the critical body parts of head, chest, upper leg; an injury criteria of Head Injury Criterion (*HIC*), Thorax Cumulative 3ms Acceleration (C_{3ms}) and peak loads of femur, respectively. Because of various parameters and constraints of initial conditions and injury thresholds, a multi-objective optimization design problem considered these main injury criterion is solved in order to achieve the best solution for this study. The results of optimized design parameters for each cases and conditions were obtained and the possibilities of the proposed concept were discussed.

Key words: Heavy Goods Vehicle(HGV), Pedestrian Safety, Collision Damage Estimation, Multi-Objective Optimization, MADYMO

1. Introduction

Research on vehicle structures to protect pedestrian injury at the collision is one of a highly important issue in vehicle safety design. Vehicle manufacturers have to meet the safety legislations and regulations in order to sell vehicles to the public. An early design stage planning with consideration of pedestrian safety is an inevitable demand and the use of computer simulation techniques such as the multi-body simulation and the finite element simulation is vital to evaluate the behavior of a real accident.

According to the type of vehicle safety system, it can mainly be divided into passive and active systems. The active system is a system that assists a driver to avoid collision such as antilock brake system (ABS), while the passive system is a vehicle component that prevents or reduces injury when a collision happens such as between an airbag and bumper. Both systems have already led to high standard protection system, but the defense for pedestrians is quite poor. Moreover, little improvement can be found in the interaction between Heavy Goods Vehicle (HGV) and pedestrians. The HGV can be defined as a truck or a lorry that has gross combination mass of over 3,500 kg. Its characteristic of

*Received 7 Feb., 2012 (No. 12-0101)

[DOI: 10.1299/jamdsm.6.541]

Copyright © 2012 by JSME

having high frontal aggressivity and large mass created serious injuries risks, if collision with pedestrian occurs. In addition, the HGV front design can be classified as flat-front type vehicle⁽¹⁾, where the front characteristic can be analogized as a straight wall. This situation assumes that all vehicle front components will hit each part of pedestrian body almost simultaneously. However, this condition should be treated differently from the bonnet-front vehicle such as automobiles, where the pedestrian will be hit at leg first, before the pedestrian is struck on the front bonnet and windscreen afterwards. Hence, for the pedestrian safety design of HGV, it is crucial to design a full frontal structure from the top to the bottom part of HGV.

Additionally, the bumper of HGV is also different from the bumper of automobiles. The HGV bumper is generally designed and manufactured by considering the compatibility between vehicle to vehicle crashes⁽²⁾. The bumper is usually the first component that interacts with pedestrian body, so the bumper energy absorber has a main role in damping the pedestrian impact and reducing the injury. In addition, a bumper could also influence the post impact kinematics of pedestrian by hitting the pedestrian lower leg. A recent ingenious solution of automobile passive system is a utilization of additional component in bumper called lower bumper stiffener (or lower absorber). The stiffener was intended to keep the bending angle of leg lower and also to reduce tibia acceleration. The idea of equipping this kind of bumper to the HGV has been preliminary analyzed in Ref.(3) and from the findings, varying bumper height and bumper protrusion would influence the lower leg injuries. However, the findings also showed that this variation gave a minimal improvement to the pedestrian's upper injuries. Therefore, an improvement to the front panel of HGV is necessary such as equipping an airbag to improve the overall result of HGV-pedestrian interaction.

So far, only a small number of researches have been performed in this field of pedestrian collision involving the HGV. Chawla et al.⁽⁴⁾, Kajzer et al.⁽⁵⁾, Longhitano et al.⁽⁶⁾ and Shen et al.⁽⁷⁾ have studied on the effect of pedestrian impacts with flat front vehicle. In addition, studies by Advanced Protection Group (APROSYS) have proposed a few possible designs of HGV passive system. Feist et al.⁽⁸⁾ have suggested a retrofittable and energy absorbing design to the front of HGV to minimize the pedestrian injury. Furthermore, Hamacher et al.⁽⁹⁾ presented a concept design of tapered shape in front of HGV. This design had been proved numerically and experimentally that it would be able to reduce injuries and able to prevent a risk of run over.

Pedestrian body can sustain a limited impact load before undergoing mechanical and physiological changes. Standard injury parameters have been recommended by recognized bodies such as EuroNCAP to identify the limitation of injury mechanism. For head injury, usually the Head Injury Criterion (*HIC*), which is a measure of the possibility of head injury occurred from an impact, is utilized. The *HIC* equation is stated as follows;

$$HIC_{15} = \left\{ \left[\frac{1}{t_2 - t_1} \int_{t_1}^{t_2} a dt \right]^{2.5} (t_2 - t_1) \right\}_{\max} \quad (1)$$

where t_1 and t_2 are the initial and final times (in seconds) of the interval during which the *HIC* attains a maximum value, and acceleration a of head is measured in g. The maximum time duration of *HIC* $t_2 - t_1$, is usually limited to 15 ms. The maximum value for *HIC* is expected less than 1,000. While the thorax, which is the next most critical organs after the head is measured by a common criterion, the Thorax Cumulative 3 ms Acceleration (C_{3ms}). C_{3ms} can be defined as the highest acceleration level that is exceeded during at least 3 ms. The maximum linear acceleration of 60 g is measured at upper thorax⁽¹⁰⁾. For upper leg injuries, a peak force value acted on left femur, F_L and right femur, F_R must be less than 10 kN⁽¹⁰⁾.

In order to reduce the whole body injuries of pedestrian, one effective solution is to perform crash simulation in high performance computer with acceptable accuracy and efficiency. Nonlinear Finite Element Analysis (FEA) such as MADYMO (Mathematical Dynamical Model) has been widely utilized for the design of vehicle but the implicit relation could affect the possibility to apply to the real application. A successful option is to apply metamodel techniques such as the response surface method (RSM). Redhe and Nilsson⁽¹¹⁾ found that the RSM performs well if the design variables are fewer and could be useful in vehicle frontal structure optimization and Fang et al.⁽¹²⁾ found that conventional quadratic polynomials do provide a good approximation to the RSM model of the energy absorption. In addition, vehicle crashworthiness involves various design variables that might conflict each other and some problems arise when a great number of design variables are involved. Hence, a multi-objective optimization could be used to solve the problem simultaneously. In the frontal impact protection, Hong et al.⁽¹³⁾ solved *HIC*, chest acceleration, chest deflection, and peak loads of femurs where the quadratic response surfaces were applied.

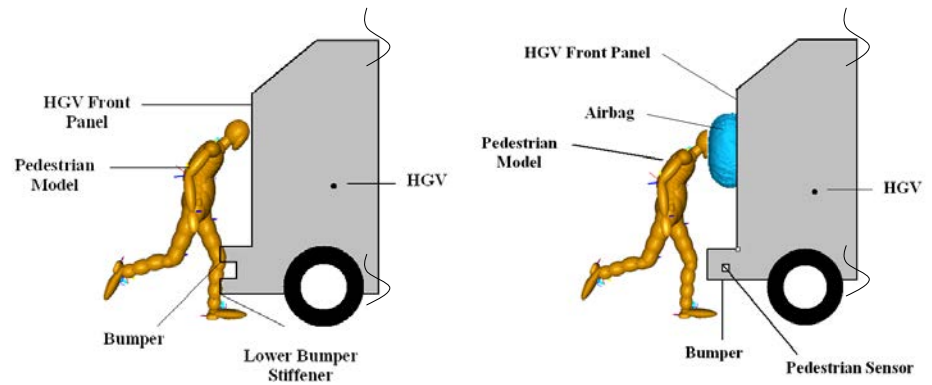
With the purpose of minimizing pedestrian injuries during collision with HGV, a multi-objective optimization using the RSM can be conducted by computer simulation. In the simulation setup, two types of models, i.e. HGV front model and pedestrian model, need to develop before a collision between the two models can be conducted. Firstly, for the HGV model, the design parameters and the design constraints that might influence the minimization of pedestrian injuries need to be identified and modeled. Furthermore, initial conditions of HGV such as mass and speed should also be applied to the model. On the other hand, for the pedestrian model, the pedestrian gaits and the initial pedestrian position before the collision with the HGV also need to be recognized. After that, the computer simulations need to be performed by using Design Of Experiments (DOE) techniques and as a result, the values of pedestrian injuries are obtained. The pedestrian injuries from the result of computer simulation are presented by different body region of pedestrian bodies such as *HIC*, C_{3ms} or leg injuries. By choosing the best response, satisfied regression model based on the DOE are estimated. In order to obtain the minimal value to the overall pedestrian injuries, significance weight is given to each of pedestrian injuries body region. Hence, a multi-objective optimization based on the weight of the body injuries can be performed mathematically and the best design parameters for the HGV can be obtained.

In this paper, two suggested design concepts of HGV, in which a lower bumper stiffener structure and an add-in airbag in front of front panel, respectively, were adopted. These designs were intended to minimize the injuries of pedestrian in the multi-body MADYMO environment by adoption of the RSM techniques with the Latin Hypercube Sampling (LHS) and the quadratic regression. The design problems were solved by multi-objective optimization to obtain the optimized lower bumper stiffener parameters and the airbag parameters, where the pedestrian injuries such as *HIC*, C_{3ms} , left and right femur loads, F_L and F_R are taken as the objective functions. The scope of this study is only focused on the duration of impact between pedestrian model of male and female with a vehicle model, respectively. Therefore, the results of this study will only be limited to the interaction of HGV and human model cases and this will ignore all the post impact cases such as impact of pedestrian with road or vehicle run-over.

2. Design Model Description

2.1 Concept of HGV-Pedestrian Protection

Two design concepts of passive pedestrian protection against collision of Heavy Gross Vehicle (HGV) are considered in this research. Figure 1(a) shows Design Concept 1, which



(a) Concept 1 – Lower bumper stiffener

(b) Concept 2 - Attached airbag

Figure 1 Design concepts for pedestrian protection against HGV

is the concept of lower bumper stiffener that has been used in some car to keep pedestrian's leg bending angle lower and also to reduce tibia acceleration. However, comparing to the collision of passenger's automobile with a pedestrian, the time duration of HGV impact with the pedestrian upper bodies are generally shorter than the time duration of the passenger's automobile. In order to delay the impact time, the bumper of HGV is equipped to project forward. In this concept, a HGV has a bumper and lower bumper stiffener mounted to the front end of the vehicle front body. During a collision, the bumper and the lower bumper stiffener of HGV will hit the pedestrian legs first, before the HGV front panel will hit the pedestrian upper bodies. By varying the bumper and the lower bumper stiffener far and closer to the ground, and the bumper and the lower bumper stiffener projected forward and backward, reducing effect of leg injuries and upper body injuries were considered.

Whereas, in the Design Concept 2 in Fig.1(b), an airbag is equipped on the HGV front panel to expect reduction of the upper bodies injuries. In this concept, a HGV has a bumper, an airbag, a pedestrian sensor and an inflator. The bumper is mounted to the front end of the vehicle front body while the airbag is located in the front end of the front panel of HGV. The sensor detects a collision between a pedestrian and the HGV, and it generates a crash signal. When the inflator receives the signal, and it responds by producing and supplying gas in order to expand the airbag. The airbag expands forward to cover the front area of the front panel and protect the upper injuries of pedestrian. Finding the combination of best airbag parameters is necessary in this design concept.

2.2 Crash Simulation in MADYMO Environment

In this study, adult pedestrians of male and female were intended to survive at a frontal impact crash of Heavy Goods Vehicle (HGV) at the maximum speed of less than 20 km/h. In order to achieve this target, two kinds of design concepts stated in the previous section were considered as case studies and treated independently. The first design concept was to see how the variation parameters of bumpers and lower bumper stiffener could influence the pedestrian injuries. While the next, second design concept was considered in which the airbag attached to the front panel of HGV is effective. All crash simulations were implemented by using MADYMO solver developed by TNO Automotive. The pedestrian models were provided by MADYMO. Most serious collision between vehicles and pedestrians occurs when pedestrian is facing sideways with the front surface of HGV. Because of this reason, only lateral impact of HGV-pedestrian was selected in this study.

For the first design concept, the frontal enhancement of HGV by means of equipping lower bumper stiffener to the front panel and without an airbag such as depicted in Fig.2

The front of HGV was developed as three rigid bodies of ellipsoids of front panel, bumper foam and lower bumper stiffener. The front panel ellipsoid was assumed to perform as an HGV front components such as grille and hood. In the real HGV design, the front panel has different value of stiffness throughout the front HGV. However for these cases, the front panel of HGV was simplified and treated to have the same stiffness so that the impact between the HGV and the upper bodies of pedestrian are the same throughout the study. The HGV windshield was ignored in this study since it was assumed that the height of the windshield was high enough that no contact occurs with pedestrian during impact. In addition, the force-displacement curve for the HGV front structure from Ref.(4) was implemented in the study and shown in Fig.3. Since the lower bumper stiffener had not been used in the HGV before, a car bumper and lower bumper stiffener from Ref.(14) are used in this study. An estimated force-displacement for both of the bumper and lower bumper stiffener such as Fig.3. The EPP foam (20 g/l in density) shown in Table 1 was selected as the materials of lower bumper stiffener. The force-displacement characteristics used for the ellipsoids were kept constant throughout the study. In addition, the location of bumper is positioned at 500 mm above the ground and 100 mm in front of the front panel surface, while, the position of lower bumper stiffener is maintained at a distant of 250 mm under the bumper.

On the other hand, for the second design concept, the same HGV model setup such as Fig.2 was implemented but added an airbag positioned at the front panel of HGV. Furthermore, the reason to use the same bumper and lower bumper stiffener for the second design concept was to observe the effect of airbag to pedestrian upper body injuries. A front passenger's MADYMO airbag model was implemented to the setup which was designed by the finite elements model. The initial location of airbag had been estimated which was by positioning it in front mid-center line of HGV front panel and locating it at 1.5 m above the ground. The airbag model setup and theory can be referred in the MADYMO Theory Manual⁽¹⁵⁾. Practically, the idea of inserting an airbag to the HGV front is quite difficult to accomplish because of the needs of a shorter airbag firing time. However, this study assumed that a short firing time could be achieved in the near future.

Furthermore, a total mass of 5,000 kg was also assigned to these bodies of HGV and the vehicle speed was set to 20 km/h. Since the pedestrian models were ellipsoid models, a multi-body to multi-body contact between the front of HGV and the pedestrian model was used. In contrast, the multi-body to the finite element contact was applied between the airbag component and the pedestrian model. Contacts between pedestrian with other surface such as ground were ignored, since the post impact study was not considered.

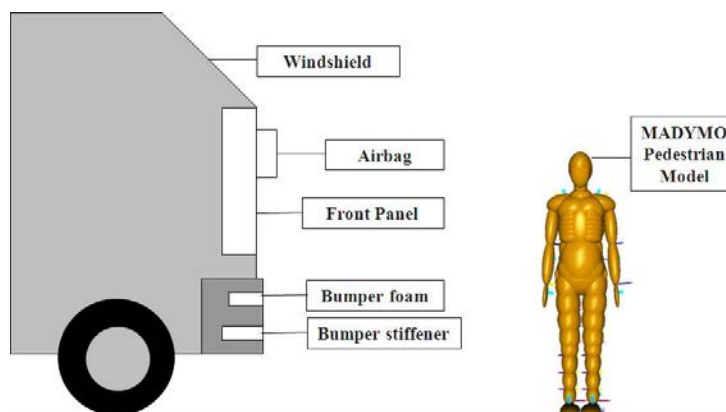


Figure 2 HGV-Pedestrian model setup

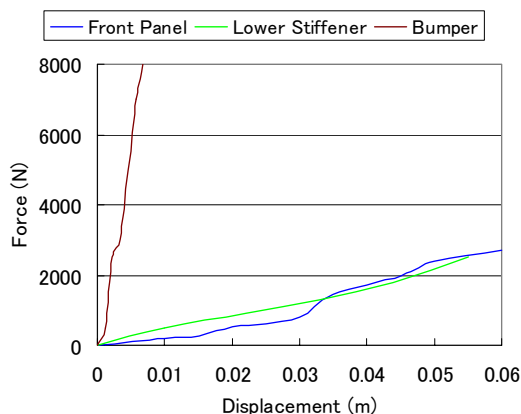


Figure 3 Stiffness of HGV front structure

Table 1 EPP foam properties

Physical properties	Values
Density (g/l)	20
Tensile strength (MPa)	0.26
Tensile elongation (%)	14
Tear strength (kN/m)	1.74
Flexural strength (MPa)	0.21
Flexural modulus (MPa)	9.8

Based on this HGV model setup, the optimum parameters of bumper and lower bumper stiffener and also airbag parameters that can minimize the pedestrian injuries were interested. In this study, the bumper foam and bumper stiffener were varied their positions to and fro, and also moving them downwards and upwards from the initial position. These parameters identified as bumper protrusion l and bumper height h were varied between -50 mm to 50 mm and between -100 mm to 100 mm, respectively. While for the airbag, after the screening procedure of airbag parameters, two variables were considered for the design optimization study; the airbag's discharge coefficient C_{Dex} , which can be defined as a scale factor area of airbag vent hole, were modified its value by increased and decreased the scale factor value by $\pm 10\%$. Furthermore, the location of airbag in z -direction was adjusted by ± 100 mm in order to observe the effect of airbag impact with pedestrian upper injuries. The other airbag parameters were maintained from the basic MADYMO airbag setup and moreover the airbag firing time was assumed at 0.002 s. Figure 4 illustrates the locations of these parameters study, while summarization of parameters is listed in Table 2.

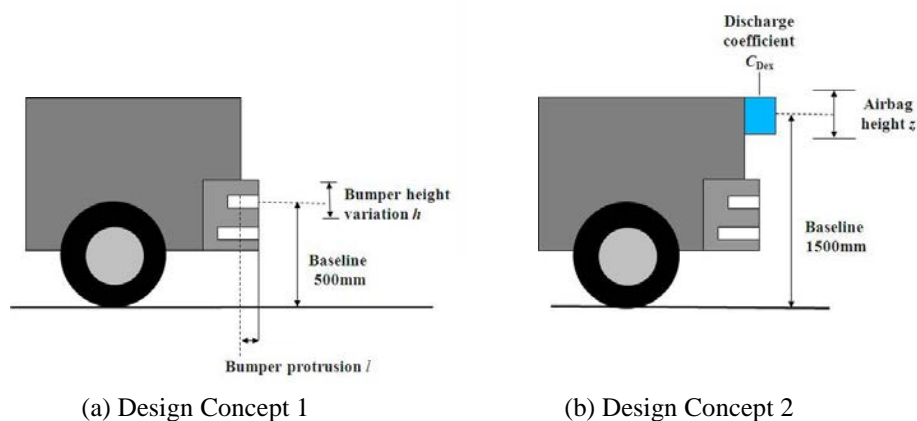
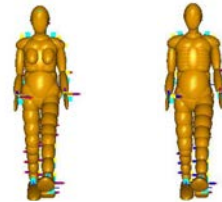


Figure 4 HGV bumper variables of Concept 1 and airbag parameters of Concept 2

Table 2 Bumper stiffener and airbag parameters

Concept	Design variable	Minimum	Nominal	Maximum
Concept 1	Bumper height h (mm)	-50.0	0.0	+50.0
	Bumper protrusion l (mm)	-100.0	0.0	+100.0
Concept 2	Discharge coefficient C_{Dex}	0.9	1.0	1.1
	Airbag height z (mm)	-100.0	0.0	+100.0



(a) Small female (b) Large male
Figure 5 MADYMO pedestrian models

Table 3 Size of pedestrian model

	Small female	Large male
Height (m)	1.53	1.74
Weight (kgW)	49.8	75.5

Table 4 Pedestrian joints modification

Stride	Angle (°)
Elbow joints	45
Shoulder joints	8.0
Right hip joint	-11
Right knee joint	22
Right ankle joint	-20
Left hip joint	22
Left knee joint	20
Left ankle joint	9.0

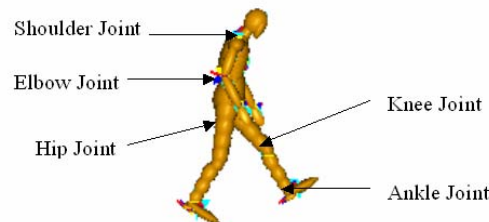


Figure 6 Pedestrian walking posture model

On the other hand, the pedestrian in the simulations were realized by two MADYMO pedestrian adult models, i.e a male model and a female model shown in Fig. 5. The MADYMO pedestrian model is an ellipsoid human model developed by TNO Automotive, and the model was built based on the data of Western European population aged 18-70 years in 1984. The height and weight of the adult models are tabulated in Table 3. Each pedestrian model is developed by 52 rigid bodies and is described by 64 ellipsoids to replicate the human bodies. The ellipsoids of the model act as several individual body parts such as head, torso or upper leg where the stiffness, shape, size, mass and inertia are predefined based on the study by MADYMO. Several joints existed such as shoulder joints and elbow joints to connect these ellipsoids together. In addition, the pedestrian model can measure the injuries loads acted on the bodies if any external impact acted on it. The MADYMO pedestrian models have been validated extensively in various studies which can be referred in the MADYMO Human Models Manual⁽¹⁵⁾. In order to used the MADYMO pedestrian model, the initial position and orientation of pedestrian of the study need to be established first. Then in the MADYMO simulations, the joints of the pedestrian model are changed in the ways to mimic the pedestrian conditions. For example, if the pedestrian is running before colliding with a vehicle, the pedestrian leg joints angles and hand joints angles before the collision need to be identified first. Then the same angle values are applied to the joints of MADYMO pedestrian model.

A study by Anderson et al.⁽¹⁶⁾ demonstrated that the walking posture of the pedestrian before collision with vehicle front influences the pedestrian kinematics and the pedestrian injuries after the impact. However, because of the highly scattered data that it might generate, the kinematics of pedestrian model was kept the same throughout the experiments in this study. The pedestrian's initial posture from Ref.(17) was assumed to be in walking

pattern with speed of 2.2 km/h and at 50% period of gait cycle. Figure 6 and Table 4 show the pedestrian model of joint states of shoulder, elbow, hip, knee and ankle that was modified according to Ref.(17). Furthermore, the pedestrian position with respect to the HGV location would be assumed to be facing the vehicle laterally in two conditions, i.e. facing left and facing right, and it was positioned exactly in the middle of the front vehicle. Due to the unsymmetrical gait of pedestrian, it is worthy noting that the pedestrians' gaits were different between both of the facing directions, and this would result in different value of injury responses between both of pedestrian positions.

All of the performed simulations were measured by the peak value output of the four main injuries. For the upper injuries of pedestrian, the peak value of Head Injury Criterion (*HIC*) and Thorax Cumulative 3ms Acceleration (C_{3ms}) were selected, while the lower injuries of pedestrian were identified by the maximum value of left femur force and right femur force. This study also only considered the condition during impact, and for this reason the pedestrian injuries at post impact cases were not observed.

Overall, four different cases of situation were conducted for Design Concept 1 of added lower bumper stiffener and another four different cases of situation were conducted for Design Concept 2 of an added airbag. To discuss easily the results in the following section, Table 5 summarizes the different cases and different pedestrian conditions, from which the Design Concept 1 was treated as Case 1 to Case 4 depending on the adult models and their facing direction and the Design Concept 2 as Case 5 to Case 8 in the following.

Table 5 Cases and pedestrian conditions

Cases	Pedestrian conditions
Case 1 (Concept 1), Case 5(Concept 2)	Male model, Facing left
Case 2(Concept 1), Case 6(Concept 2)	Male model, Facing right
Case 3(Concept 1), Case 7(Concept 2)	Female model, Facing left
Case 4(Concept 1), Case 8(Concept 2)	Female model, Facing right

3. Optimum Design Problem Definition

A general optimization problem for both of design concepts stated in the previous section can be express as follows;

$$\text{Minimize injury} \quad F(\mathbf{x}) = [\text{Head injury criterion } (HIC), \text{ Cumulative thorax 3ms acceleration } (C_{3ms}), \text{ Peak force of right femur } (F_R), \text{ Peak force left femur}(F_L)]$$

$$\begin{aligned} \text{Subject to} \quad & HIC \leq 1,000 \\ & C_{3ms} \leq 60 \text{ (g)} \\ & \text{Peak force of right femur, } F_R \leq 10 \text{ (kN)} \\ & \text{Peak force of left femur, } F_L \leq 10 \text{ (kN)} \end{aligned}$$

$$\begin{aligned} \text{For Design Concept 1} \quad & -50 \text{ (mm)} \leq h \leq 50 \text{ (mm)} \\ & -100 \text{ (mm)} \leq l \leq 100 \text{ (mm)} \end{aligned}$$

For Design Concept 2, the following constraints are added,

$$\begin{aligned} & 0.9 \leq C_{Dex} \leq 1.1 \\ & -100 \text{ (mm)} \leq z \leq 100 \text{ (mm)} \end{aligned} \quad (2)$$

4. Solving Method

The Response Surface model Method (RSM) approximates highly complicated objective and constraint functions involved in the design problems. Figure 7 presents the response surface model method with multi-objective optimization employed in this study. Firstly, the optimization problem including the objectives, constraints and design variables is defined. A set of sampling points is selected based on Latin Hypercube Sampling (LHS) and computed in the MADYMO FEA environments. The MADYMO peak results of pedestrian injuries are obtained as the responses. These data points and responses are then used to construct the quadratic regression models to approximate the FEA solutions and then the fitting accuracy of the models is validated. If the accuracy is not satisfied, a new regression model should be constructed by additional new sampling points. Afterwards, multi-objective optimization is performed with weight values assigned to the responses to obtain the best design solutions for the problems.

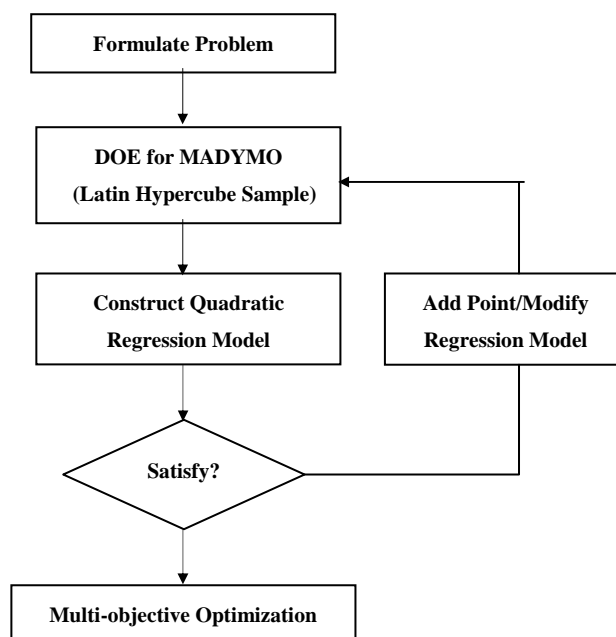


Figure 7 Flowchart of multi-objective optimization

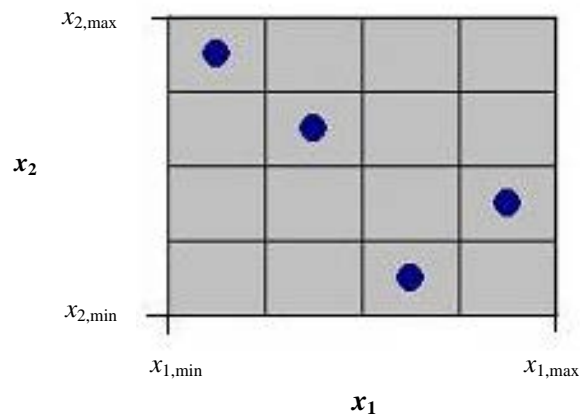


Figure 8 Latin Hypercube sampling

4.1 Latin Hypercube Sampling

Among the Design Of Experiments (DOE) techniques, the Latin Hypercube Sampling (LHS) technique shown in Fig. 8 is used to construct the response surface models for the crashworthiness criteria of vehicle. The LHS is a type of space filling design which spreads the design points nearly evenly throughout the region of experiments. An example in Fig. 8 shows a generation of sample size, $N=4$ and 2 variables $x=(x_1 \text{ and } x_2)$. The range of x_1 and x_2 are divided into 4 equal intervals vertically and 4 equal intervals horizontally, and producing a total of 16 cells that cover the overall sampling space. Sampling points are then generated at random manner in non-overlapping intervals by pairing the values of x_1 and x_2 . For this example, a total of 4 sampling points are formed evenly. The number of runs in the LHS is set in the beginning of the experiments and can vary according to the availability of computing resources. Hence, for complex and time-consuming problems, it is preferable to use fewer samples. For this reason, a set of 10 sampling points is applied to the HGV-Pedestrian study with consideration of 2 variables for each design concepts.

For the Design Concept 1, the bumper height h and bumper protrusion l were set as variables and by pairing the values of h and l , 10 sampling points were generated using the LHS. The generated sampling points were then used in conducting the computer simulations of HGV-Pedestrian. By changing the values of h and l based on the sampling points in the HGV model, 10 different simulations of HGV-Pedestrian collision were conducted in the MADYMO for each Case 1 to Case 4. From the results of the simulations, the values of pedestrian injuries of HIC , C_{3ms} , F_L and F_R were obtained and were employed in the construction of the quadratic regression model.

In the same ways, the LHS technique was used in generating sampling points for the Design Concept 2, in which the discharge coefficient C_{Dex} and the airbag position z were combined in generating 10 sampling points. The similar MADYMO simulations were conducted for Case 5 to Case 8 and the HIC , C_{3ms} , F_L and F_R were used in the construction of the regression model.

4.2 Quadratic Regression Model

Generally, a second order regression model is constructed to represent the physical phenomena considered in this paper and Eq. (3) were utilized in the RSM, where b_i and b_{ij} are the regression coefficients determined by least square method.

$$y(x) = b_0 + \sum_{i=1}^n b_i x_i + \sum_{i=1}^n b_{ij} x_i + \sum_{i=1}^n b_{ij} x_{ij} \quad (3)$$

Statistical analysis techniques can be used to check the fitness of response surface model. The usual statistical parameter used for evaluating model fitness is a coefficient of determination R_2 , which is the statistical measure of how well a regression approximates real data points. Equation (4) below shows the formula to calculate R_2 .

$$R_2 = \frac{\sum_{i=1}^n (\hat{y}_i + \bar{y}_i)^2}{\sum_{i=1}^n (y_i + \bar{y}_i)^2} \quad (4)$$

where n is the number of design points and \hat{y} , y and y_i represent the predicted response, the mean of the responses and the actual response, respectively. An R_2 of 1.0 (100%) indicates a perfect fit. Thus, the higher the value of R_2 is, the more accurate and the better the fit data is.

Table 6 Significance body region injuries⁽¹⁸⁾

Body Region	Significance	Weights
Head	60%	$W_1 = 0.6$
Chest	35%	$W_2 = 0.35$
Extremities (Legs)	5%	$W_3 = 0.05$

4.3 Multi-objective Optimization Technique

The satisfied quadratic model for each HIC , C_{3ms} , F_L and F_R obtained for each Case 1 to Case 8 are able to solve the Equation (2) individually by mathematical programming. However, due to the possibilities of design parameters conflicting the pedestrian injuries, multi-objective optimization for all these injuries were conducted. Because the collision involved the whole pedestrian bodies, the significance injuries such as states in Table 6 is considered. Hence, the weighted injury criterion, WIC in Equation (5) is useful by combining these four injury criteria as a single-design objective⁽¹⁸⁾.

$$WIC = 0.6 \left(\frac{HIC}{1000} \right) + 0.35 \left(\frac{C_{3ms}}{60g} \right) + 0.05 \left(\frac{F_R + F_L}{20kN} \right) \quad (5)$$

To solve the variables value of h and l for the Design Concept 1 and the variables value for C_{Dex} and z for the Design Concept 2, the multi-objective optimization solutions were solved using desirability functions⁽¹⁹⁾ built in Minitab software.

Generally for each case, the individual response values of HIC , C_{3ms} , F_L and F_R are transformed using a specific desirability function into a single objective. The individual desirability for each response, d_i are calculated as follows:

$$d_i = f_i(y)^W \quad (6)$$

where W is the significance weight for HIC , C_{3ms} , F_L and F_R defined in Table 6 and $f_i(y)$ are used to minimize the response by

$$f_i(y) = \frac{(U_i - y_i)}{(U_i - L_i)} \quad (7)$$

where y_i , U_i and L_i are the response value, upper limit and lower limit of HIC , C_{3ms} , F_L and F_R , respectively. The weighted composite desirability, D is calculated as

$$D = (d_1 * d_2 * \dots * d_n) \quad (8)$$

Continuous value of d_i was calculated based on the quadratic model for each of HIC , C_{3ms} , F_L and F_R by substituting the variables h and l continuously for the Design Concept 1 or C_{Dex} and z for the Design Concept 2. The highest value of D was chosen when these variables were solved.

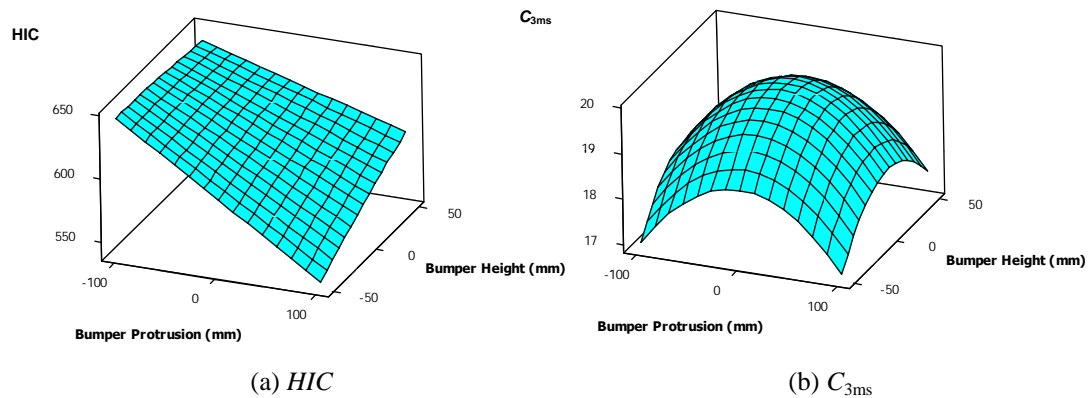


Figure 9 Response surface plots for bumper height h and bumper length l

Table 7 Results of coefficient of determination R^2

Parameters	<i>HIC</i>	C_{3ms}	F_L	F_R
Case 1	0.993	0.887	0.989	0.769
Case 2	0.901	0.708	0.947	0.819
Case 3	0.999	0.733	0.929	0.997
Case 4	0.998	0.789	0.992	0.787
Case 5	0.993	0.835	0.665	0.901
Case 6	0.942	0.835	0.866	0.611
Case 7	0.865	0.959	0.850	0.977
Case 8	0.888	0.792	0.743	0.912

5. Results and Discussions

5.1 Accuracy of Regression Model

For each case, the second order response surface models for pedestrian injuries of HIC , C_{3ms} , F_L and F_R had been developed from the simulation response results using the Latin Hypercube Sampling points. For example in Case 1, the model of HIC is constructed as

$$HIC = 11.69h^2 - 36.55l^2 + 14.77hl + 11.68h - 36.55l + 603.84 \quad (9)$$

where h (mm) is bumper height and l (mm) is bumper protrusion. The plotted HIC and C_{3ms} surface models are illustrated in Fig. 9.

The models were tested to see whether the data were well fitted in model or not. The calculated R^2 values for HIC of the Design Concept 1 are 0.993, 0.901, 0.999 and 0.998 for Case 1 to Case 4, respectively. These results are accurate enough because that the HIC data for the response are well fitted in the developed models. The similar situations can be observed for the other values of R^2 as summarized in Table 7. The values of R^2 for the other models are moderately less accurate. From these results, it is found the regression models for this research are considered adequate.

5.2 Multi-objective Optimization Results of Concept 1

Table 8 represents the results of the optimization for the four cases of simulations by varying the location of bumper and lower bumper stiffener of Design Concept 1. The results

Table 8 Results of optimal design for Concept 1 (Single Case)

Conditions	Optimal design variables	Min <i>HIC</i>	Min <i>C</i> _{3ms} (g)	Min <i>F</i> _L (kN)	Min <i>F</i> _R (kN)	Min <i>WIC</i>
Case 1	<i>l</i> = 100mm , <i>h</i> = -50 mm	560.1	19.10	0.447	0.643	0.450
Case 2	<i>l</i> = 100mm , <i>h</i> = -50 mm	557.1	17.34	0.410	0.561	0.437
Case 3	<i>l</i> = -100 mm , <i>h</i> = -50mm	824.7	19.55	0.845	0.819	0.613
Case 4	<i>l</i> = -100 mm , <i>h</i> = -11.8 mm	625.2	24.19	0.425	1.271	0.520

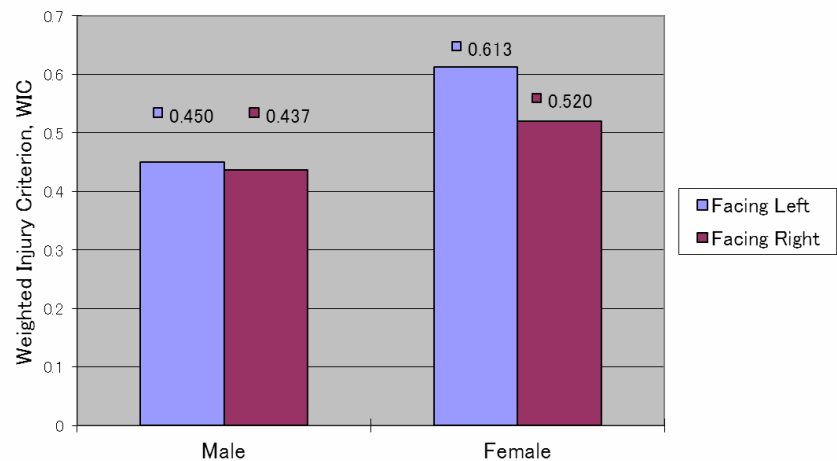


Figure 10 Results of *WIC* for Concept 1

represents all cases with the values of optimal design variables, the minimum values of *HIC*, *C*_{3ms}, *F*_L and *F*_R injuries and also the total value of weighted injury criterion, *WIC*.

Observing each single case, the lowest values of *WIC* were obtained when the bumper is lower from the initial position. For Case 1 to Case 3, the optimum bumper height *h* is -50mm, while for Case 4, the optimal bumper height *h* is -11.8mm. Whereas, by moving the bumper forward to 100 mm, the lowest values of *WIC* for Case 1 and Case 2, were attained. However, for Case 3 and Case 4, the optimal bumper protrusions *l* was located at -100mm from initial position. Due to the multi-objective optimization, the different *WIC* results are probably affected by the conflicting value of the injuries. Because the leg injuries only influence the *WIC* by 0.5%, the values of *WIC* would most likely affected by the value of *HIC* and *C*_{3ms}.

Considering optimum injuries for each case, the *HIC* and *C*_{3ms} and both the *F*_L and *F*_R values attained the safer values under the threshold. For each Case 1 to Case 4, the minimum values of *HIC* are 560.1, 557.1, 824.7 and 625.2, respectively. On the other hand, the optimum *C*_{3ms} injuries are 19.1 g, 17.3 g, 19.6 g and 24.2 g, respectively. In addition, lower values of peak force acted on both *F*_L and *F*_R were acquired, where all cases have the optimum values between 410 N to 1.271 kN. The lower value of *F*_L and *F*_R can be explained by the use of a car bumper in these experiments, in which it is softer comparing to the bumper of a real truck. The value of *WIC* is also less than 1.0, which means that both of the adult models are able to survive against the collision of front lateral impact with a speed 20 km/h.

Figure 10 shows the *WIC* for all four cases. By comparing the results, all *WIC* values for each case are different. In addition, the *WIC* value for male model is slightly lower than the female model. This is true since the male model is stronger. Moreover, by comparing the two different gait cycles, the *WIC* for male model was almost the same, while the female

Table 9 Results of optimal design for Concept 1 (Combined Cases)

Conditions	Optimal Design Variables	Min <i>HIC</i>	Min <i>C</i> _{3ms} (g)	Min <i>F</i> _L (kN)	Min <i>F</i> _R (kN)	Min <i>WIC</i>
Case 1	<i>l</i> = -100 mm , <i>h</i> = -16.6 mm	636.9	19.06	1.593	1.376	0.501
Case 2		698.8	21.74	1.193	1.037	0.552
Case 3		826.6	20.63	0.762	0.770	0.620
Case 4		634.3	23.36	0.404	1.285	0.521

model has different *WIC* values. For female model, different optimal values of *h* and *l* might results to a different value of *WIC*. However for male model, although both of the optimal values of *h* and *l* are same, different minimum values of injuries of *HIC*, *C*_{3ms}, *F*_L and *F*_R are acquired and this resulted to the different calculation of *WIC*. Because of this difference, it can be said that the gait cycle of pedestrian model influences the results of *WIC*.

In order to see the single optimal solution to design variables for all conditions when the adult models of male and female hit laterally by the HGV at 20 km/h, all these four cases were optimized by combined all the injuries responses. Table 9 represents the optimal parameters of *h* and *l*, the pedestrian injuries parameters and the result of *WIC* for each case.

The optimum bumper protrusion *l* attained is -100mm from initial position and the optimum bumper height *h* attained was slightly lower -16.6 mm to the ground. Also from Table 9, all the *WIC* values were increased due to this optimization comparing to the values of *WIC* for a single case (Table 8). This is especially for Case 1 and Case 2, in which the head injuries and leg injuries are increased. However, the *HIC*, *C*_{3ms}, *F*_L, *F*_R and the *WIC* values are still under the threshold values.

In general, the concept of adjusting the position of bumper and lower bumper stiffener could influence the result of pedestrian injuries. Although different cases give different optimum value of injuries, the optimum solutions for the design problems still manage to be obtained. However, from the conducted simulations and optimizations, upper injuries such as head injury and chest injury had the most influence toward the obtained result. Hence, protection to the upper part of pedestrian is more necessary in the HGV-Pedestrian collision. Because of this reason, an airbag attached to the front panel of HGV is more desirable.

5.3 Optimization of Airbag

All the results of the four simulation cases of Design Concept 2 are presented in Table 10. Based on the results obtained, in general, a height increase of airbag position from the ground would be lower value for the *WIC*. Through Case 5 to Case 8, the optimal design variables *z* is 96mm, 39mm, 100mm and 100mm respectively. This can be explained by the height of both of pedestrian models where the male model height is 1.74 m, while the female model height is 1.53 m. By lowering the airbag from its initial height position of 1.50m, the airbag may not be able to protect the pedestrian's head, and for this reason will increase the values of *HIC* and *WIC*. In addition, for this study, the maximum height of 1.60 m (1.50m+100mm), maybe good enough to protect both models since Case 5 and Case 7 which are similar in gait position, has the same optimum *WIC* value. On the other hand, the value of *C*_{Dex} for each case is different from each other. There is a possibility that a small change of the vent hole size does not influence the pedestrian injuries so much comparing to the location of airbag.

For each single case, the minimum injuries attained have lower values than the value of threshold. For Case 5 to Case 8, the minimum values of *HIC* are attained as 29.2, 41.5, 25.6 and 105.9, respectively. Whereas, the optimum *C*_{3ms} injuries are 16.6 g, 16.4 g, 17.4 g and 14.7 g. Comparing to the Design Concept 1, a significant value of *HIC* and a small value of *C*_{3ms} had been improved. Since the Design Concept 2 used the same bumper and lower bumper stiffener of the Design Concept 1, a smaller optimized value of *F*_L and *F*_R had been

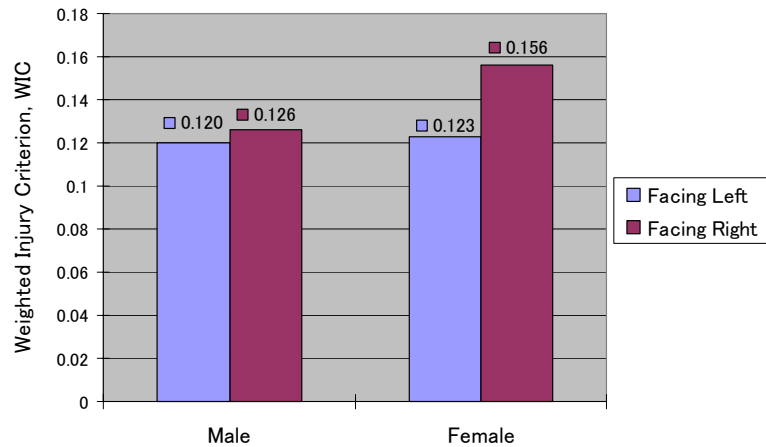


Figure 11 Result of *WIC* for Concept 2

Table 10 Results of optimal design for Concept 2 (Single Case)

Conditions	Optimal design variables	Min <i>HIC</i>	Min $C_{3ms}(g)$	Min $F_L(kN)$	Min $F_R(kN)$	Min <i>WIC</i>
Case 5	$C_{Dex} = 0.90$, $z = 96mm$	29.21	16.63	0.909	1.378	0.120
Case 6	$C_{Dex} = 0.90$, $z = 39mm$	41.51	16.39	0.750	1.584	0.126
Case 7	$C_{Dex} = 1.07$ $z = 100 mm$	25.63	17.43	0.705	1.647	0.123
Case 8	$C_{Dex} = 1.10$ $z = 100 mm$	105.9	14.73	0.621	1.773	0.156

Table 11 Results of optimal design for Concept 2 (Combined Cases)

Conditions	Optimal design variables	Min <i>HIC</i>	Min $C_{3ms}(g)$	Min $F_L(kN)$	Min $F_R(kN)$	Min <i>WIC</i>
Case 5	$C_{Dex} = 0.98$ $z = 54 mm$	40.27	17.06	0.986	1.366	0.130
Case 6		186.76	15.5	0.816	1.448	0.208
Case 7		150.58	15.4	0.681	1.746	0.186
Case 8		107.64	17.03	0.854	1.568	0.170

obtained which is less than the threshold value of 10kN.

In comparison with male and female models, Figure 11 shows the value of *WIC* for all the four cases. All cases have unique and lower *WIC* values of 0.120, 0.126, 0.123 and 0.156. However, the differences between all cases are quite small. Since head injury contributes to 60% of *WIC* calculation and the low values of *HIC* are obtained for all cases, it can be said that the obtained location of airbag is good enough to protect the head injury for both models. In comparison between the two facing conditions, higher values of *WIC* were obtained for Case 6 and Case 8 (Facing left condition). Since the position of airbag is also not the same, direct comparison between the two facing directions are unable to be performed. However, the kinematics of pedestrian during collision might influence the value of pedestrian injuries.

In addition, the single optimal solution of airbag was performed by combined all the injuries response of Case 5 and Case 8 and are presented in Table 11. The C_{Dex} value attained is 0.98 and the position of z is 54mm. However, the *HIC* values were increased due to this optimization especially for Case 6 and Case 7. Both cases have a reduced C_{3ms} values compare to the C_{3ms} values of Case 5 and Case 8. Minor changes were observed from the results of F_L and F_R . This is because of these leg injuries are mostly influenced by the impact of bumper and lower bumper stiffener, and not by the airbag. Furthermore, the

values of WIC had also increased, demonstrating that the obtained injuries for all cases and single case were different. All of the results were under the threshold values, which mean that the airbag with lower stiffener bumper is considered effectived to protect the pedestrian.

Comparing the injuries responses of pedestrians between Concept 1(Table 9) and Concept 2(Table 11), an improvement of HIC up to 15 times were achieved for Case 5. Whereas, there are only slight changes to the C_{3ms} values (40% for Case 5) and non-significant difference of values of F_L and F_R . Because of these low injury values compare to the threshold values, it was predicted that a slightly higher speed of more than 20km/h may save the pedestrian life. Overall, the concept of attaching airbag in front of the HGV in the HGV-Pedestrian collision is considered sensible to reduce overall pedestrian injuries, especially the head injuries.

6. Conclusions

In this paper, the concept of lower bumper stiffener and the concept of airbag which had been studied in the pedestrian safety of automobiles had been employed in the HGV-Pedestrian collision. These concepts were approached to discover their potential in reducing the pedestrian injuries of head, chest and legs. The Response Surface Method has been applied and a multi-objective optimization has been solved for the bumper parameters and airbag parameters in eight different cases. Based on the results,

- (1) In the lower bumper stiffener concept and the airbag concept, different values of optimal design variables and responses to the injury were obtained for each different single case. However, combinational case for these studies suggested that the bumper and lower stiffener should be moved back -100mm and lowered -16.6mm from the original position. Whereas, the values of $C_{Dex} = 0.98$ and moving the airbag upwards to 54mm is considered the best cases for airbag.
- (2) The potential of both of the lower bumper stiffener and airbag in HGV is sensible at the low speed since both of pedestrian model would be able to sustain at HGV collision with the speed 20 km/h.
- (3) The accuracy of the optimal studies for both concepts has been examined by the HIC , C_{3ms} , F_L and F_R model which have been found adequate for all cases.

References

- (1) Tanno, K., Kohno M., Ohashi N., Ono K., Aita K., Oikawa H., Myo-Thaik-Oo, Honda K. and Misawa S., Patterns and mechanisms of pedestrian injuries induced by vehicles with flat-front shape, *Legal Medicine*, Vol. 2(2) (2000), pp. 68-74.
- (2) Chinnaswamy, G.K., Chirwa, E.C., Nammi, S.K., Nowpada, S., Chen, T. and Mao, M., Benchmarking and accident characteristics of flat-fronted commercial vehicles with respect to pedestrian safety. *International Journal of Crashworthiness*, Vol. 12(3) (2007) pp. 279-291.
- (3) Ramli, F.R. and Yamazaki, K., Analysis and design of HGV front structure for pedestrian safety. *Proceedings of the JSME Design and System Conference* (2010).
- (4) Chawla, A., Sharma, V., Mohan, D. and Kajzer, J., Safer truck front designs for pedestrian impacts, *Proceedings 1998 International IRCOBI Conference on the Biomechanics of Impact* (1998).
- (5) Kajzer, J., Aldman, B., Mellander, H., Planath, I. and Jonasson, K., Safer bus fronts for pedestrian impact protection in bus pedestrian accidents: A preliminary investigation, *Proceedings 1992 International IRCOBI Conference on the Biomechanics of Impact*, (1992).

- (6) Longhitano, D., Ivarsson, J., Henary, B. and Crandall, J., Torso injury trends for pedestrian struck by cars and LTVs, *Proceedings of the 19th International Technical Conference of Enhanced Safety Vehicles Conference* (2005).
- (7) Shen, J., Jin, X.L. and Zhang, X.Y., Simulated evaluation of pedestrian safety for flat front vehicles. *International Journal of Crashworthiness*, Vol. 13(3) (2008), pp. 247-254.
- (8) Feist, F., Gugler, J., Giordab, A., Avalleb, M. and Puppini, R., Improvements to the protection of vulnerable road users: retrofittable, energy-absorbing front end for heavy goods vehicles, *International Journal of Crashworthiness*, Vol. 13(6) (2008), pp.609-627.
- (9) Hamacher, M., Fassbender, S., Fest, F. and Gugler, J., Modification of a truck front for improved kinematics in run over, *Proceedings of the 21st International Technical Conference of Enhanced Safety Vehicles Conference (ESV)*, (2009).
- (10) Federal Motor Vehicle Safety Standards and Regulations www.nhtsa.gov/cars/rules/import/fmvss/index.html
- (11) Redhe, M. and Nilsson, L., Optimization of the new Saab 9–3 exposed to impact load using a space mapping technique. *Structure and Multidisciplinary Optimization*, Vol. 27(5) (2004), pp. 411–420.
- (12) Fang, H., Solanki, K. and Horstemeyer, M.F., Numerical simulations of multiple vehicle crashes and multidisciplinary crashworthiness optimization. *International Journal of Crashworthiness*, Vol. 10(2) (2005), pp. 161–171.
- (13) Hong, J.H., Mun, M.S. and Song, S.H., An optimum design methodology development using a statistical technique for vehicle occupant safety. *Proceedings Institute Mechanical Engineering D Journal of Automobile Engineering*, Vol. 215(7) (2001) pp. 795–801.
- (14) Untaroiu, C.D., Shin, J., Crandall, J., Fredriksson, R., Bostrom, O., Takahashi, Y., Akiyama, A., Okamoto, M. and Kikuchi, Y., Development and validation of pedestrian sedan bucks using finite element simulations; application in study the influence of automatic braking on the kinematics of pedestrian involved in vehicle collision, *International Journal of Crashworthiness*, Vol. 15(5) (2010), pp.491-503.
- (15) MADYMO Theory Manual Release 7.0, TNO, (2008).
- (16) Anderson, R.W.G., Long, A.D., Serre, T. and Masson, C., Determination of boundary conditions for pedestrian collision reconstruction. *Proceedings of the ICrash Conference*, (2008).
- (17) Untaroiu, C.D., Meissner, M., Crandall, J.R., Takahashi, Y., Okamoto, M, Ito, O. Crash reconstruction of pedestrian accidents using optimization techniques. *International Journal of Impact Engineering*, Vol. 36(2) (2009), pp. 210-219.
- (18) Xingtao, L, Qing, L, Xujing, Y, Wei, L and Weigang, Z (2008) A two-stage multi-objective optimisation of vehicle crashworthiness under frontal impact *International Journal of Crashworthiness*, Vol. 13(6) (2008), pp.609-627.
- (19) Derringer, G. and Suich, R., Simultaneous optimization of several response variables. *Journal of Quality Technology* Vol. 12, pp. 214-219.